J. Fluid Mech. (1971), *vol.* 46, *part* 1, *pp.* 177–198
Printed in Great Britain

An investigation of the forces on flat plates normal to a turbulent flow

By P. W. BEARMAN†
National Physical Laboratory, Teddington, Middlesex

(Received 23 April 1970)

Measurements on square and circular plates in turbulent flow show the mean base pressure to be considerably lower than that measured in smooth flow. Power spectral density measurements of the fluctuating component of the drag on square plates in both smooth and turbulent flow are presented. The measurements in turbulent flow show the importance of the ratio of turbulence scale to plate size. There is shown to be a strong correlation between the fluctuating drag force and the velocity fluctuations in the approaching flow. The distortion of the turbulence structure approaching a plate is also discussed.

1. Introduction

Many flow environments are turbulent and these are not always well simulated by the smooth flow usually found in wind tunnels. The flow in the earth's boundary layer, for example, is highly turbulent and this will influence the response of flexible buildings and structures. In order to be able to determine this response it is important that the effects of turbulence on the flow around bluff bodies should be clearly understood. The object of this paper is to examine the relationship between the approaching turbulent flow and the mean and fluctuating forces on a series of flat plates set normal to this flow. The paper concentrates on the effects of turbulence and does not discuss the effects of mean shear.

A body placed in a uniform turbulent stream can be affected in a number of ways, the most obvious of which is the production of fluctuating forces by the approaching fluctuating velocities. The mean flow and mean forces can also be affected because turbulence can promote transition in boundary layers and free shear layers at lower Reynolds numbers than those normally found in smooth flow. A turbulent stream will also influence the growth of boundary layers and wakes. Schubauer & Dryden (1935) were the first to notice that turbulence increased the mean drag of flat plates. Measurements of the mean base pressure on a series of square and circular plates are discussed in § 3.2 of this paper. The effects of both intensity and turbulence scale have been examined and their influence on mean base pressure is considered in § 3.3.

The measurements of the fluctuating component of the drag force on square plates in turbulent flow are presented in § 3.5. This particular shape of body was

† Present address: Aeronautics Dept., Imperial College, London, S.W. 7.

chosen because it was hoped that there would be no regular vortex shedding and that the major part of the fluctuating drag force would be directly related to the approaching turbulent flow. Davenport (1961) has suggested the use of a frequency-dependent transfer function, relating fluctuating force to the longitudinal component of fluctuating velocity, called aerodynamic admittance. Measurements of the aerodynamic admittance of flat plates have been reported by Wardlaw & Davenport (1964) and Vickery (1965), but agreement between the two sets of measurements is poor. One of the aims of the present research was to carry out a more systematic investigation of aerodynamic admittance with particular attention being paid to the importance of the ratio of turbulence scale to plate size. A discussion of the aerodynamic admittance results is given in §3.6.

In §3.7 the structure of the turbulent flow ahead of a plate is discussed. The extent of the correlation between the fluctuating drag force and the fluctuating velocity (indicated by a hot wire positioned at various distances ahead of the plate) was measured. The concept of aerodynamic admittance requires this correlation to be high. In addition to the effect of the turbulence on the plates there will be some effect of the plates on the stream turbulence. Hunt (1970) has proposed a theory to analyze the distortion of the turbulence in the flow past a body. The measurements of turbulence structure are discussed in the light of Hunt's findings.

2. Experimental arrangement

The experiments were conducted in a wind tunnel with a 9 ft (2·74 m) × 7 ft (2·13 m) by 12 ft (3·66 m) long working section. The tunnel is of the closed-return type and has a free-stream turbulence level of about 0·2 % and a top speed of 200 ft/sec (61 m/sec). A highly turbulent flow was generated by the installation of a square-mesh grid at the beginning of the working section. The grid, which was of the bi-planar type, was constructed from 1·5 in. × 0·75 in. (3·81 cm × 1·9 cm) wooden slats spanning the tunnel and the distance between the centres of slats, the mesh size, was 7·5 in. (19 cm). With the grid in position, the efficiency of the fan dropped to about 50 % and the maximum speed of the tunnel was reduced to 100 ft/sec. The flow behind the grid is discussed in §3.1.

The flow was examined around square plates of side 2, 3, 4, 6 and 8 in. (5·08, 7·61, 10·16, 15·22 and 20·3 cm) and circular plates of 4 and 7 in. (10·16 and 17·77 cm) diameter. Pressure measurements were made using an Infra-red Development micromanometer and the electrical output from the manometer was integrated to obtain a time mean value of pressure. For the examination of the effect of turbulence on mean base pressure, the plates were attached to a string supported on a movable frame. The effect of intensity was examined by positioning the plates at various distances x, downstream of the grid, and the effect of turbulence scale was mainly examined by working with different sizes of plate.

Mean and fluctuating forces were sensed by a semi-conductor strain-gauged drag balance having two strain-gauged links, one on each side, and these were 0·1 in. (2·54 mm) long, 0·075 in. (1·91 mm) wide and 0·010 in. (0·254 mm) thick.

These gauges formed two arms of a bridge and the two dummy gauges completing the bridge were attached to the body of the balance. The balance is discussed in more detail by Bearman (1969). The plates were supported on a light, hollow, tapered sting 18 in. (0·457 m) long. The sting was protected from the airflow by a fibre-glass shroud attached, at the balance end, to the earthing frame. The shroud tapered from $\frac{7}{8}$ in. (2·22 cm) diameter down to $\frac{5}{8}$ in. (1·59 cm) at the model. Transverse oscillations of the sting and model were eliminated by placing a thin strip of foam rubber around the end of the sting, between it and the shroud. The lowest natural frequency of the balance, with the sting and a 4 in. square plate attached, was about 1·5 KHz.

The whole assembly was supported on a massive I-beam bolted to a concrete bed beneath the tunnel. The support system was so positioned as to place the plates at 6·33 ft (1·93 m) downstream of the turbulence grid. The lowest natural frequency of the support system was about 200 Hz but oscillations of the support system were extremely small and only a very small apparent drag signal resulted from this vibration. The power spectra of the drag were smoothed across this very narrow frequency range.

The balance was calibrated with the sting vertical and, with applied dead-weight loads up to 2 lbf (8·9 N), no departure from linearity was observed. The balance was mainly sensitive to axial load and extremely insensitive to any bending moment applied to the string. With the 4 in. square plate attached to the sting a load was applied at the centre of the plate and then at each corner. The largest variation in the output only represented a difference of 0·7 % of the load applied at the centre.

The bridge circuit was not temperature-compensated and the output of the balance showed a strong temperature dependence. The sensitivity of the balance, working in a constant-current mode, only changed by about 0·1 %/C. The zero, however, drifted by about 10 % of full-scale reading per degree Centrigrade, thus making the accurate measurement of mean drag force difficult. The drift of the zero was found to be fairly well correlated with the temperature of the air in the neighbourhood of the active gauges. During a run this temperature was continuously monitored by a thermocouple. Initially runs were made with the sting removed and with the balance completely sealed in order to estimate the dependence of zero drift on ambient temperature. For the determination of mean drag coefficient, correction was made to allow for this zero drift.

Turbulence measurements were made with DISA constant-temperature hot-wire anemometers. Fluctuating velocity and fluctuating drag signals were recorded on an AMPEX FR 1300 tape recorder and, except where indicated, these signals were later digitized and analysis was performed on a KDF-9 digital computer.

3. Experimental results and discussion

3·1 *Flow behind the turbulence producing grid*

The variation of the intensity $(\overline{u^2})^{\frac{1}{2}}/U$ and the longitudinal integral scale Lx of the streamwise component of turbulence behind the grid, along the centre-line

of the working section, is shown in figure 1. These measurements were made using an unlinearized hot-wire anemometer and the scale was estimated from spectra measured on a third-octave spectrum analyzer. At the plate position adopted

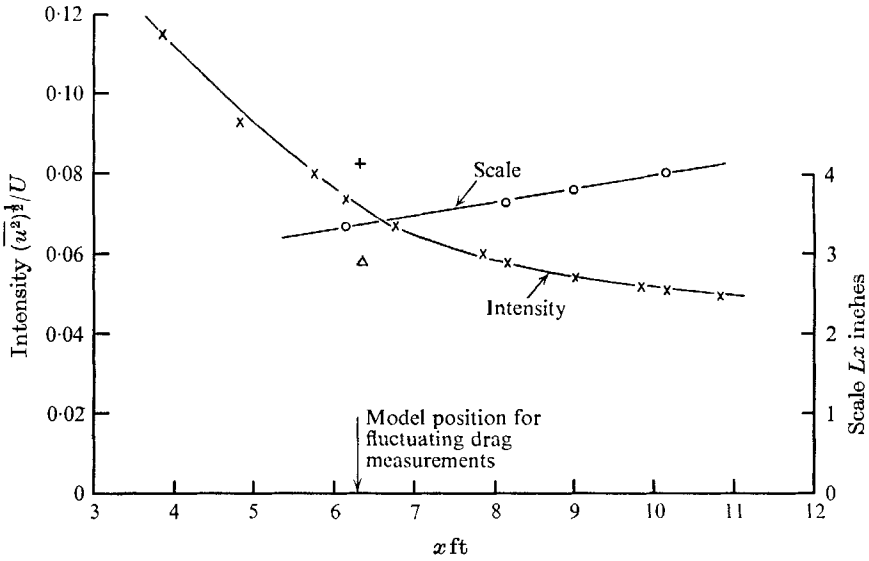

FIGURE 1. Variation of intensity and scale of 'u' component of turbulence along working section centre-line (U = 40 ft/sec). ×, intensity; ○, scale; unlinearized anemometer. +, intensity; △, scale; linearized anemometer.

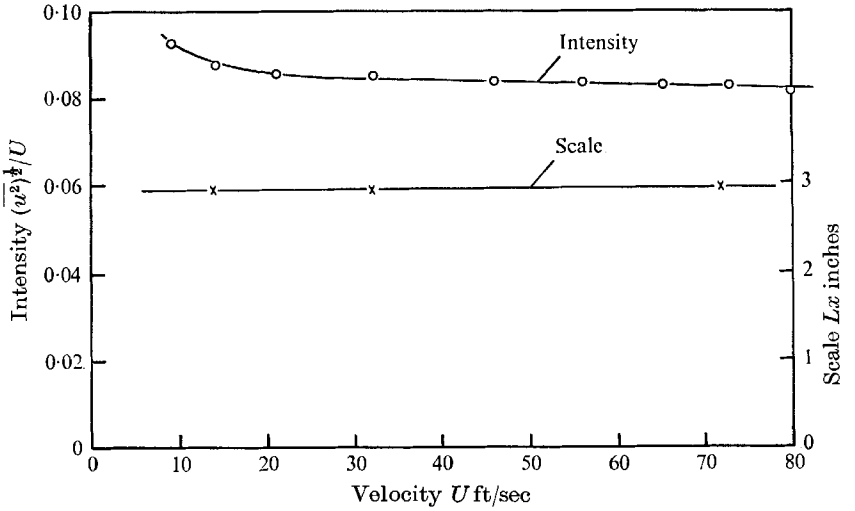

FIGURE 2. Variation of turbulence intensity and scale with velocity at 10·1 mesh lengths from the grid (the test position). ○, intensity; ×, scale.

for the fluctuating drag measurements the turbulence was investigated more carefully, with a linearized hot-wire anemometer and the values of intensity and scale are also shown in figure 1. This position, 10·1 mesh lengths from the grid, will be referred to as the test position. The main reason for the discrepancy

between the two sets of readings was the limited low frequency response of the instrument used to measure the r.m.s. voltage fluctuation indicated by the unlinearized anemometer. In order to keep the signal to noise ratio of the drag balance high the test position had to be in a region of high turbulence intensity

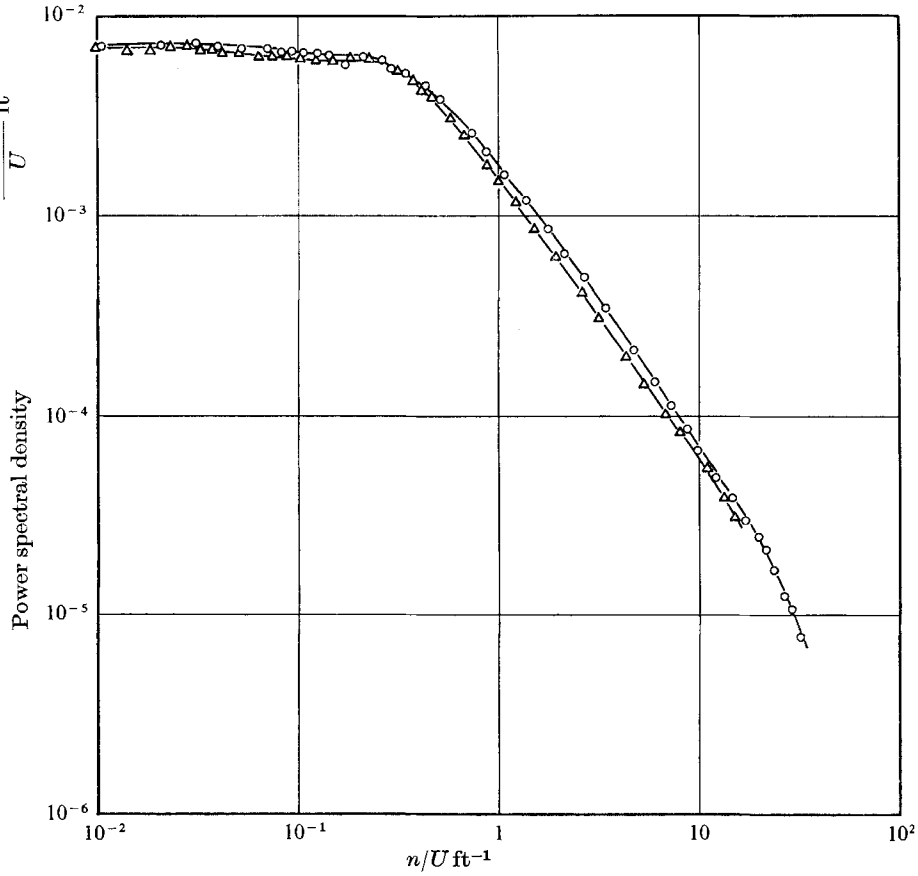

FIGURE 3. Spectra of longitudinal component of turbulence at test position. ○, $U = 32$ ft/sec; △, $U = 72$ ft/sec.

close to the grid. At the test position, over the area to be occupied by the plates, the mean velocity and the intensity of turbulence were found to be uniform to within $\pm 0{\cdot}30\,\%$. At a fixed distance x from the grid the turbulence intensity decreased very slightly with increase of tunnel speed. Figure 2 shows the variation of intensity and scale with velocity at the test position. Spectra of the 'u' component of turbulence, measured at two wind speeds at the test position, are shown in figure 3. X-probe measurements showed the turbulent energy to be approximately equally distributed among its three components.

3.2. *Measurement of mean base pressure*

The first part of the investigation consisted of the measurement of mean base pressure on the plates in smooth flow. In this paper smooth flow is to be interpreted as the flow in the tunnel in the absence of any turbulence producing

grids (i.e. $(\overline{u^2})^{\frac{1}{2}}/U = 0{\cdot}002$). Figure 4 shows the base pressure distribution on the 8 in. square plate measured from a line of tappings running across half the rear face of the plate. The pressure is presented in the form of a pressure coefficient $(C_p)_b$, where $(C_p)_b = (p_b - p)/\frac{1}{2}\rho U^2$ and p_b is base pressure and p and U are respectively free stream static pressure and velocity. These results have been corrected for the effects of wind-tunnel blockage using the method of Maskell (1965). The pressure across the base is seen to be nearly uniform and all further base pressure coefficients presented were determined from the pressure at the position $y/D \doteq 0{\cdot}2$.

$(\overline{u^2})^{\frac{1}{2}}/U = 0{\cdot}083$, $Lx = 3$ in. (7·62 cm).

Plate size (in.)	C_D		$-(C_p)_b$	
	Smooth	Turbulent	Smooth	Turbulent
2 × 2	1·120	1·260	0·363	0·505
4 × 4	1·090	1·220	0·363	0·46
6 × 6	1·107	1·195	0·363	0·431
8 × 8	1·152	1·175	0·363	0·410

TABLE 1. Comparison of mean drag coefficient of flat plates in smooth and turbulent flow

The results from all the plates in smooth flow, over a range of Reynolds number, showed a good collapse. The values of $(C_p)_b$ for the circular plates were found to be the same as those for square plates. These results showed that base pressure was independent of Reynolds number, over the range to be investigated in turbulent flow. All plates were tested with the same sting and therefore the collapse of results suggests that the size of the sting relative to the plate size had a negligible effect on the mean base pressure readings. The corrected values of $(C_p)_b$, given in table 1, agree closely with previous measurements of Fail, Lawford & Eyre (1955) at a similar Reynolds number.

Figure 4 also shows the base pressure distribution across the 8 in. square plate in turbulent flow, at a position where $(\overline{u^2})^{\frac{1}{2}}/U = 0{\cdot}083$ and $Lx/D = 0{\cdot}375$ (D is plate width), and it can be seen that there was a marked decrease in base pressure suggesting an increase in drag. Base pressure coefficients measured in turbulent flow, for all the plates, are shown in figure 5 plotted against the distance from the grid x/M. For each plate size, at a given position, there was no variation of $-(C_p)_b$ with Reynolds number. The smaller plates had the higher values of $-(C_p)_b$ and these values varied little with distance from the grid. In turbulent flow, pressure coefficients were formed using the time mean values of free stream static pressure and velocity.

3.3. *Discussion of mean base pressure results*

At these Reynolds numbers, in smooth flow, transition in the free shear layer springing from a plate occurs very soon after separation and the resulting turbulent shear layer rapidly entrains fluid from the base cavity formed by the

separated flow. This entrainment of fluid from the cavity sustains the low base pressure. In a turbulent stream it can be expected that there will be some extra entrainment due to the more vigorous mixing of the wake with the external

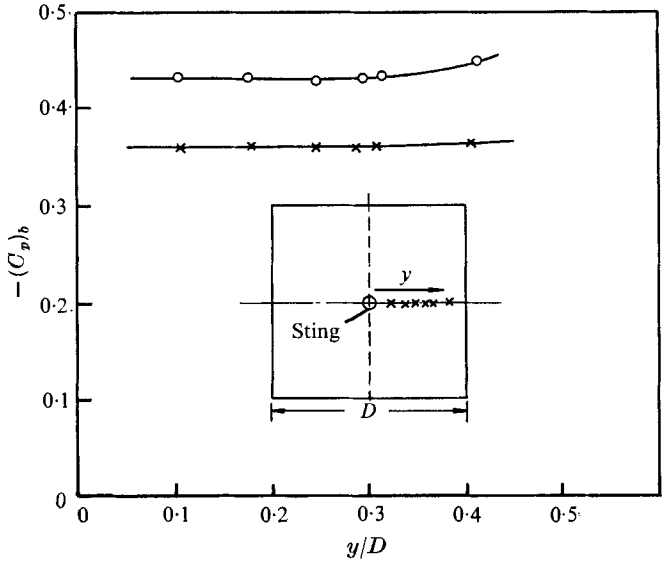

FIGURE 4. Base pressure distributions on 8 in. × 8 in. plate in smooth and turbulent flow, $R = 2 \times 10^5$. ×, smooth flow; ○, turbulent flow, $Lx/D = 0{\cdot}375$ and $(\overline{u^2})^{\frac{1}{2}}/U = 0{\cdot}083$.

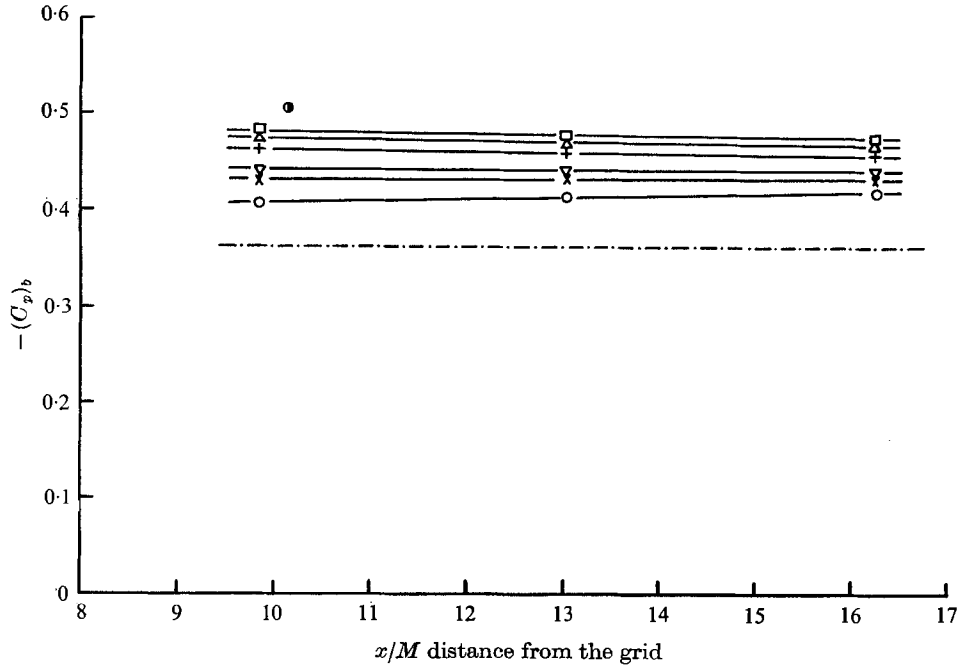

FIGURE 5. Base pressure measurements on flat plates in turbulent flow. Reynolds number range $0{\cdot}48 \times 10^5$ to $2{\cdot}14 \times 10^5$. ◑, 2 in. × 2 in.; □, 3 in. × 3 in.; +, 4 in. × 4 in.; ×, 6 in. × 6 in.; ○, 8 in. × 8 in.; △, 4 in. dia.; ▽, 7 in. dia.; —·—·—·, smooth flow results.

flow. Explorations with a hot wire suggested that, in turbulent flow, the shear layer leaving the plate was laminar but that transition occurred at about the same distance downstream. Transition occurred very abruptly and was marked by a burst of turbulence of a much higher frequency content than that of the surrounding ambient turbulent flow. It is argued that the principal effect of the external turbulent flow is the extra entrainment of fluid out of the wake.

The rate m at which turbulence can entrain fluid from an adjoining undisturbed fluid is set by the scale and intensity of its energy-containing eddies. The scale of these energy-containing eddies is related to the integral scale Lx. Thus

$$m = F(\rho, \mu, Lx, (\overline{u^2})^{\frac{1}{2}})$$

and

$$\frac{m}{\rho Lx^2 (\overline{u^2})^{\frac{1}{2}}} = F\left(\frac{\rho(\overline{u^2})^{\frac{1}{2}} Lx}{\mu}\right). \tag{1}$$

Since the effect of turbulence Reynolds number is expected to be small, the turbulent entrainment rate is proportional to $\rho Lx^2(\overline{u^2})^{\frac{1}{2}}$. It is now assumed that equation (1) also approximately describes the extra entrainment process in the near wake of the flat plates. In turbulent flow the base pressure $p_b - p$ can be described by

$$p_b - p = F(\rho, \mu, U, D, m),$$

so that

$$\frac{p_b - p}{\frac{1}{2}\rho U^2} = F\left(\frac{\rho UD}{\mu}, \quad \frac{m}{\rho UD^2}\right). \tag{2}$$

Base pressure has been found to be independent of Reynolds number and, therefore, using the result of (1)

$$(C_p)_b = F\left(\frac{Lx^2}{D^2}\frac{(\overline{u^2})^{\frac{1}{2}}}{U}\right). \tag{3}$$

The base pressure coefficient is shown plotted against the turbulence parameter $[(\overline{u^2})^{\frac{1}{2}}/U]\,Lx^2/A$, where A is plate area, in figure 6. It is interesting to note that even quite small values of $[(\overline{u^2})^{\frac{1}{2}}/U]\,Lx^2/A$ give substantial departures from the so-called smooth air value. In the smooth flow, for the 2 in. plate $[(\overline{u^2})^{\frac{1}{2}}/U]\,Lx^2/A$ was approximately 5×10^{-4}.

It cannot be expected that, as Lx^2/A becomes very large, $-(C_p)_b$ will also become very large. When the size of the energy containing eddies becomes much larger than the size of the body, their main effect will no longer be to mix with the wake flow but to cause an effect similar to that of a slowly varying mean velocity. Under such conditions the drag in turbulent flow C_{DT} is related to the turbulence intensity by

$$C_{DT} = C_D\left(1 + \frac{\overline{u^2}}{U^2}\right), \tag{4}$$

where C_D is the drag coefficient measured in smooth flow. Therefore the relationship in (3) will only apply where Lx is less than, or of the same order as, the size of the largest eddies in the wake. In the experiments reported here $(\overline{u^2})^{\frac{1}{2}}/U$ was less than 0·1 and therefore the maximum increase in drag, due to this rectification effect, would not be greater than 1 %. Figure 5 shows that, for each plate size, the

base pressure coefficient was sensibly independent of distance from the grid. Equation (3) suggests, therefore, that the turbulence parameter

$$[(\overline{u^2})/U^{\frac{1}{2}}](Lx/M)^2$$

is also independent of distance from the grid and the measurements confirm this.

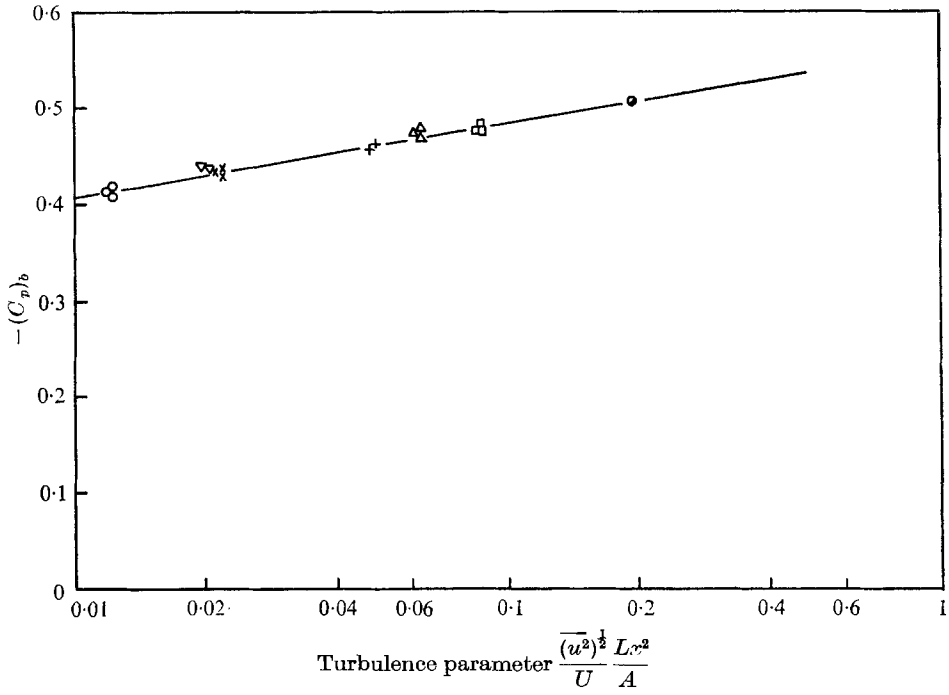

FIGURE 6. Base pressure coefficients in turbulent flow ◑, 2 in. × 2 in.; □, 3 in. × 3 in.; +, 4 in. × 4 in.; ×, 6 in. × 6 in.; ○, 8 in. × 8 in.; △, 4 in. dia.; ▽, 7 in. dia.

3.4. *Measurement of mean drag*

When mounted on the drag balance the plates were positioned 10·1 mesh lengths from the grid, where $(\overline{u^2})^{\frac{1}{2}}/U = 0{\cdot}083$, and it was only possible to investigate the effect of scale on mean drag. Drag coefficients were calculated from values of the drag force integrated over a suitable time period. Corrections were made to allow for the effects of any temperature drift during this period and for the effect of wind-tunnel blockage. The corrected values of mean drag ceofficient are shown in table 1 for both smooth and turbulent flows. The accuracy of the results is thought to be no better than about $\pm 3\,\%$ and the inaccuracy is reflected in the scatter of the C_D values measured in smooth flow. Nevertheless, it can be clearly seen that, in turbulent flow, C_D varied in the same manner as $-(C_p)_b$. On a flat plate, in smooth flow, only just over 30 % of the drag results from the low pressure on the rear face. In turbulent flow it is to be expected that the front face pressure distribution will only be slightly modified and therefore, although in some cases $(C_p)_b$ changed by as much as 30 %, the mean drag coefficient only varied by about 10 %.

3.5. *Measurement of fluctuating drag*

The fluctuating drag component of the square plates (of side 2, 4, 6 and 8 in.) was measured over a range of Reynolds number. The power spectral density estimates of all the drag signals are plotted together in figure 7. This graph shows the power spectral density estimate of the fluctuating drag coefficient $F(C_D)(n)$

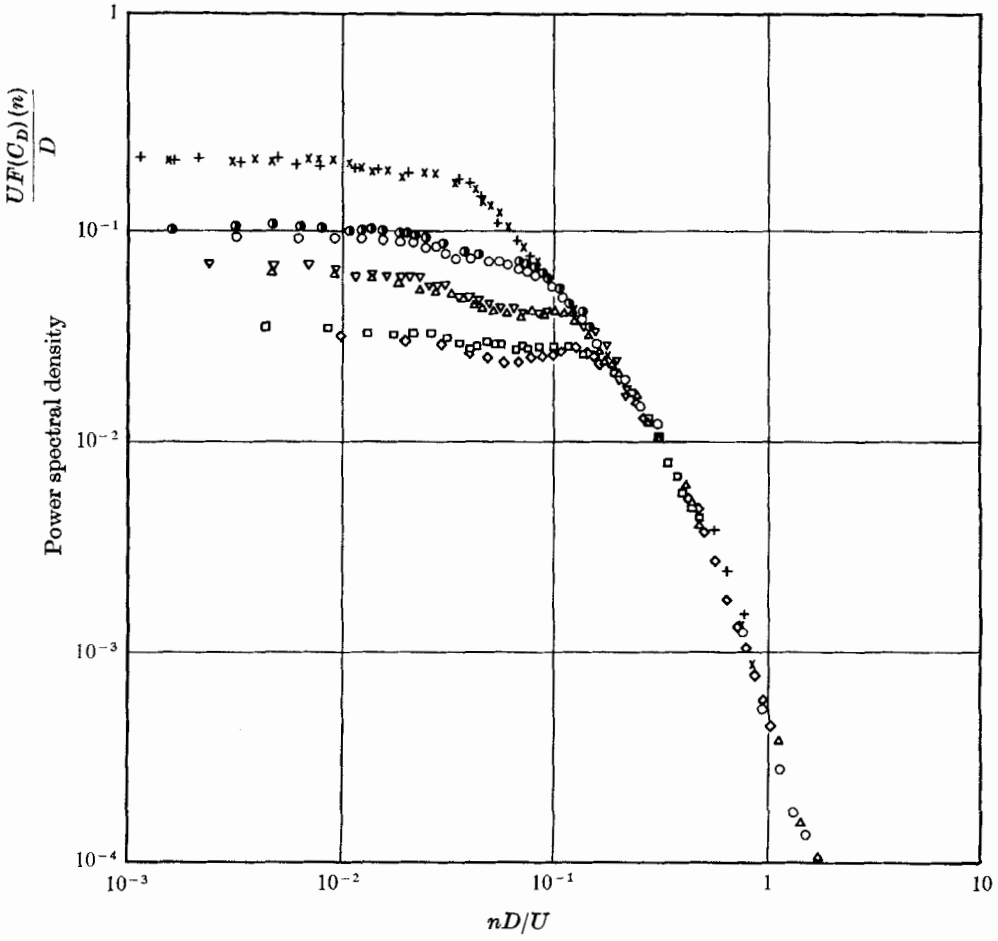

FIGURE 7. Spectra of the unsteady component of drag of flat plates in turbulent flow ($Lx = 3$ in., $(\overline{u^2})^{\frac{1}{2}}/U = 0{\cdot}083$). ×, 2 in. × 2 in., $R = 0{\cdot}69 \times 10^5$; +, $R = 0{\cdot}98 \times 10^5$; $Lx/D = 1{\cdot}5$. ○, 4 in. × 4 in., $R = 0{\cdot}70 \times 10^5$; ◑, $R = 1{\cdot}39 \times 10^5$; $Lx/D = 0{\cdot}75$. △, 6 in. × 6 in., $R = 1{\cdot}04 \times 10^5$; ▽, $R = 2{\cdot}08 \times 10^5$; $Lx/D = 0{\cdot}50$. □, 8 in. × 8 in., $R = 0{\cdot}88 \times 10^5$; ◇, $R = 1{\cdot}96 \times 10^5$; $Lx/D = 0{\cdot}375$.

at frequency n, plotted as the non-dimensional quantity $UF(C_D)(n)/D$ against the non-dimensional frequency parameter nD/U. All measurements were made at the test position where $(\overline{u^2})^{\frac{1}{2}}/U = 0{\cdot}083$ and $Lx = 3$ in. (7·6 cm). For each plate size the results show little dependence on the Reynolds number. The measurements illustrate the importance of the parameter Lx/D, the ratio of the integral scale of the turbulence to the size of the plate.

Since

$$(C_{D\text{r.m.s.}})^2 = \int_0^\infty \frac{UF(C_D)(n)}{D}\, d\left(\frac{nD}{U}\right),$$

where $C_{D\text{r.m.s.}}$ is the root-mean-square value of the coefficient of the fluctuating component of drag, it is clear that the smallest plate has the largest mean-square drag coefficient. This is primarily because, on the smaller plates, the correlation areas of the energy-containing eddies of the turbulence are comparatively larger.

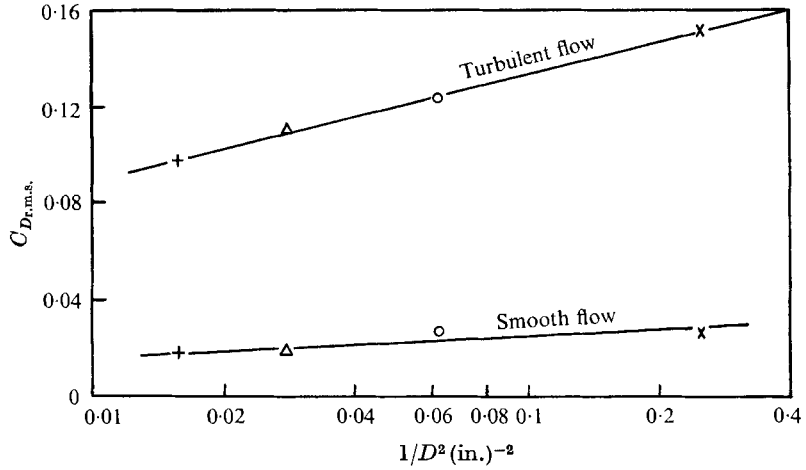

FIGURE 8. R.m.s. of drag coefficient fluctuations of flat plates in smooth and turbulent flow. ×, 2 in. × 2 in.; ○, 4 in. × 4 in.; △, 6 in. × 6 in.; +, 8 in. × 8 in.

There are two possible length scales that could be used to non-dimensionalize the results shown in figure 7, plate size or turbulence scale. The data are shown non-dimensionalized by plate dimension D and in this case the variation of the parameter Lx/D can equally well be thought of as being due to a plate of fixed size in a turbulent stream of fixed intensity and varying scale. Increasing the scale of turbulence, while the intensity remains constant, will have the effect of increasing the power spectral density at long wavelengths and decreasing the power spectral density at short wavelengths. This effect is manifest in the spread of results for the various values of Lx/D (shown in figure 7) at low values of nD/U. If the results had been non-dimensionalized by Lx instead of D there would have been a much closer collapse of the data at long wavelengths and a spread at shorter wavelengths. The r.m.s. values of fluctuating drag coefficient are shown in figure 8 plotted against $1/D^2$. It can be expected that the fluctuating drag will be a function of both $(\overline{u^2})^{\frac{1}{2}}/U$ and Lx/D and, since $(\overline{u^2})/U$ and Lx were constant in this experiment, it seemed most appropriate to plot drag against the inverse of the plate area.

An interesting feature of the spectra in figure 7 is the collapse of the data on to a single curve at high values of nD/U. Since the data are non-dimensionalized by plate dimension it suggests that, at these values of nD/U, the drag is not directly related to the approaching turbulence spectrum but is, perhaps related to wake-induced pressure fluctuations on the rear face. In order to obtain some

ideas on the contribution from the rear face the fluctuating drag was measured on the plates in smooth flow. The power spectral density estimates of fluctuating drag coefficient in smooth flow are plotted in figure 9. The r.m.s. values were very

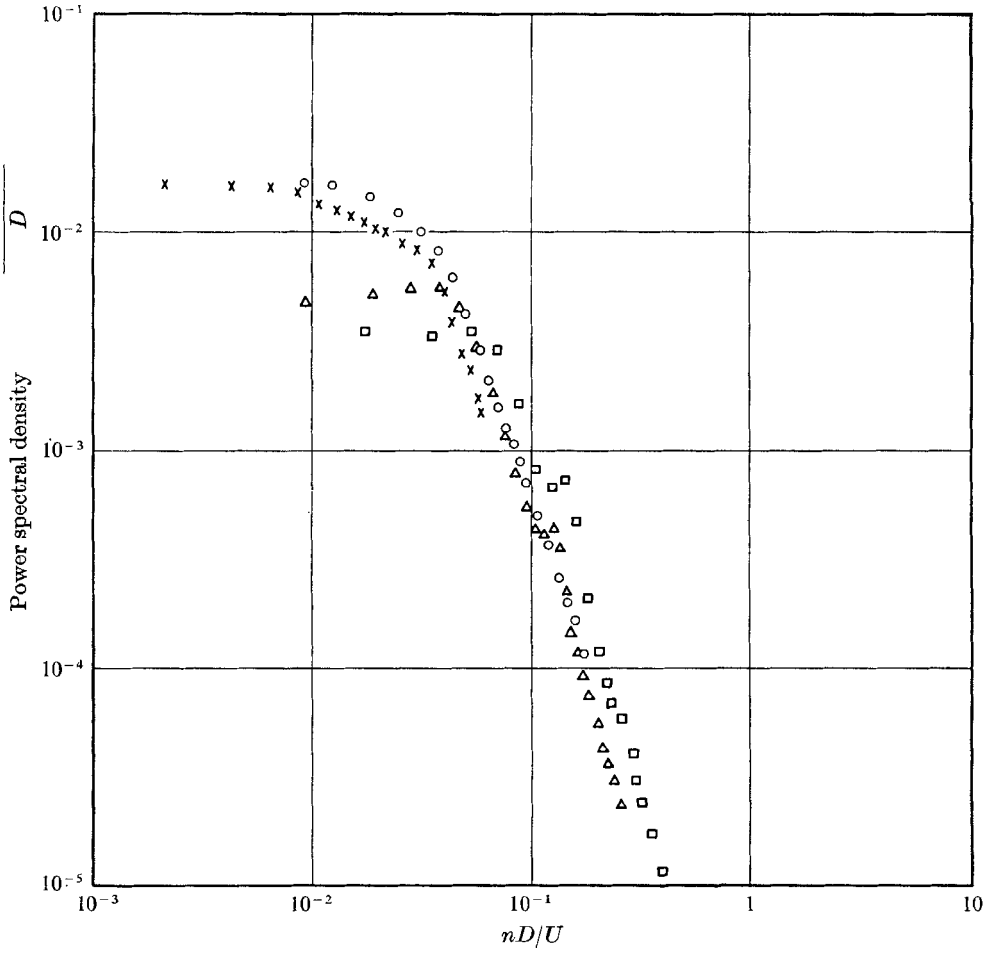

FIGURE 9. Spectra of the unsteady component of drag of flat plates in smooth flow. ×, 2 in. × 2 in., $R = 10^5$, $U = 93{\cdot}6$ ft/sec; ○, 4 in. × 4 in., $R = 1{\cdot}37 \times 10^5$, $U = 64{\cdot}2$ ft/sec; △, 6 in. × 6 in., $R = 2{\cdot}06 \times 10^5$, $U = 64{\cdot}4$ ft/sec; □, 8 in. × 8 in., $R = 1{\cdot}95 \times 10^5$, $u = 45{\cdot}7$ ft/sec.

small (about 0·02) and are plotted in figure 8. With this very low level of fluctuating drag signal the r.m.s. noise to signal ratio of the balance and recording system rose to about 0·1.

The spectra show similar features to those measured in turbulent flow with a spread of the results for different plate sizes at low values of nD/U and an approximate collapse at high values. Fluctuations in drag can be caused by self-induced pressure fluctuations in the wake, tunnel turbulence and tunnel noise. The plates are not expected to experience significant drag fluctuations caused by the acoustic pressure fluctuations of the tunnel noise since the wavelengths of this noise, at these low frequencies, will be very long. The velocity fluctuations associated

with these sound waves, which are measured as part of the tunnel turbulence level, although small, will be correlated over a large area and could induce a small force on the plates. The rest of the tunnel turbulence will probably be of smaller scale and mostly emanate from the fan and honeycomb (there were no screens in the tunnel). The turbulence level varies with wind speed and the results shown in figure 9 were measured at a variety of wind speeds. This is thought to be the reason why, at low values of nD/U, $UF(C_D)(n)/D$ does not show as consistent a variation with plate size as that found in turbulent flow. The r.m.s. values of the drag coefficient in smooth flow, presented in figure 8, show a trend towards higher values at smaller plate sizes. This suggests that a proportion of the fluctuating drag was produced by tunnel turbulence. At higher values of nD/U, however, there is a rough collapse of the data and a rapid fall off in power spectral density. At these higher values of nD/U the fluctuations in drag must be mostly self-induced in the sense that they originate from the unsteady motion within the near wake of the plates. The most important result of the smooth flow experiments was the discovery that the rate of fall off of the spectra at high values of nD/U was exactly the same as that found in turbulent flow. The level of the spectra in smooth flow, however, was nearly three orders of magnitude down at the same value of nD/U.

3.6. *Discussion of fluctuating drag results*

Before discussing the effect of turbulence on fluctuating drag the simpler case of the drag of a body in a stream of varying longitudinal velocity will be considered. Equation (5), which has been suggested by several authors including Bearman (1969), shows the relationship between the power spectral density of the fluctuating component of the drag coefficient and the power spectral density of the velocity of the approaching unsteady flow.

$$F(C_D)(n) = 4C_D^2 \frac{F(u)(n)}{U^2}\left[1+\frac{C_m^2}{C_D^2}\left(\frac{2\pi nD}{U}\right)^2\right], \tag{5}$$

where C_m is the coefficient of virtual mass. This equation shows the increasing importance of the virtual mass contributions as the frequency parameter nD/U is increased.

The use of equation (5) is limited by the fact that very little information exists on the value of C_m for bluff bodies with large separated wakes. Also C_D and C_m may be frequency dependent or may depend in some way on the complete spectrum of the approaching flow. In turbulent flow equation (5) will be modified in some way by the extent of the spatial correlation of the fluctuating velocity. Davenport (1961) argues that, in turbulent flow, there will still be a linear relationship between drag fluctuations and the incident velocity fluctuations. He has termed the function $X^2(n)$ aerodynamic admittance where

$$X^2(n) = \frac{U^2F(C_D)(n)}{4C_D^2F(u)(n)}. \tag{6}$$

In the simple unsteady flow

$$X^2(n) = 1+\frac{C_m^2}{C_D^2}\left(\frac{2\pi nD}{U}\right)^2 \tag{7}$$

and at small values of nD/U, aerodynamic admittance will approach unity.

Wardlaw & Davenport (1964) and Vickery (1965) have measured the aerodynamic admittance of flat plates in turbulent flow. Following these authors, figure 10 shows $X^2(n)$ plotted against nD/U for the four sizes of square plate examined in this investigation. The value of C_D used in the calculation of $X^2(n)$

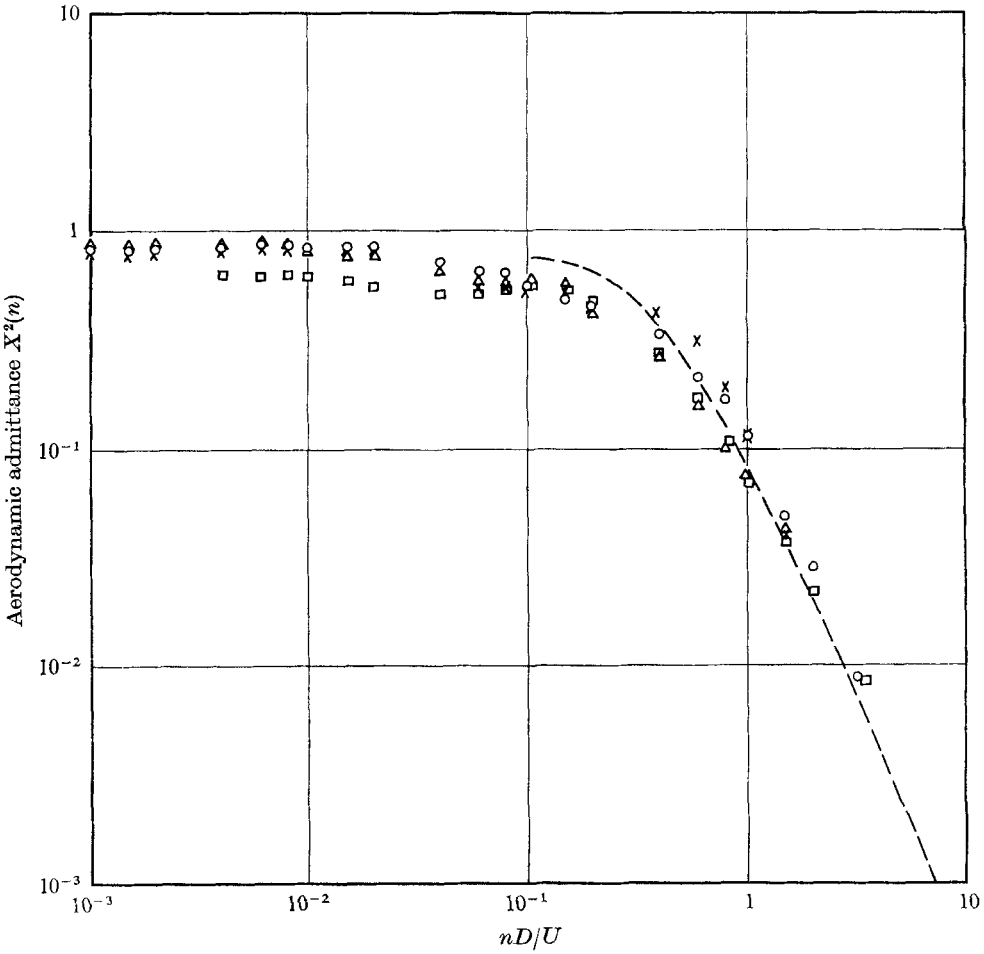

FIGURE 10. Aerodynamic admittance of flat plates. ×, 2 in. × 2 in., $Lx/D = 1{\cdot}5$; ○, 4 in. × 4 in. $Lx/D = 0{\cdot}75$; △, 6 in. × 6 in., $Lx/D = 0{\cdot}50$; □, 8 in. × 8 in., $Lx/D = 0{\cdot}375$; – – – –, Vickery, $Lx/D = 1{\cdot}05$.

is that measured in turbulent flow and presented in table 1. As nD/U tends to zero, aerodynamic admittance rises to a value less than unity. The simple unsteady theory assumed an infinite lateral correlation length for the fluctuating velocity whereas in turbulent flow, at very long wavelengths, the correlation length will be of the same order as the integral scale. Therefore it can be argued that measured values of $X^2(n)$ will be less than unity. At high values of nD/U the aerodynamic admittance drops off at a rate of about 14 dB/octave. Vickery (1965) suggests that at high values of nD/U the spatial correlation of the tur-

bulence decreases rapidly and that this will have a much stronger effect on $X^2(n)$ than the increase in the drag force resulting from the virtual mass contribution.

The measurements of $X^2(n)$ made by Vickery (1965) on a square plate in a turbulent flow of intensity 10% and with a scale approximately equal to the plate size, are also shown in figure 10 and are in agreement with the author's results. Wardlaw & Davenport's (1964) earlier measurements of $X^2(n)$, however, show substantially less agreement. Perhaps the reasons for this may be found in the accuracy of the experiments. In the words of the authors, their experiments were of an exploratory character and there were certain features of the model design that could have introduced extraneous effects on the measurements.

Vickery (1965) has formulated a theory to calculate the aerodynamic admittance of a lattice plate which has individual members small compared to the correlation lengths of the velocity fluctuations of interest. The main assumptions are that the force on a member can be related directly to the local upstream velocity and that the correlation of forces is identical to the lateral correlation of upstream velocities. For a square lattice plate Vickery finds

$$X^2(n) = \frac{1}{D^4}\int_0^D \int_0^D \int_0^D \int_0^D F(u_1, u_2)\,(r, n)\,dx_1 dx_2 dy_1 dy_2, \tag{8}$$

where $F(u_1, u_2)\,(r, n)$ is the normalized form of the lateral co-spectral density function of the longitudinal component of the oncoming turbulent flow. x_1, y_1 and x_2, y_2 are the co-ordinates of two points on the plate surface and

$$r = [(x_2 - x_1)^2 + (y_2 - y_1)^2]^{\frac{1}{2}}$$

and

$$\int_0^\infty F(u_1, u_2)\,(r, n)\,dr = Lr(n),$$

where $Lr(n)$ is the lateral correlation length of the turbulence at frequency n. It has been shown by Bearman (1969) how (8) can be re-written in the simpler form

$$X^2(n) = \frac{4}{D^4}\int_0^D \int_0^D (D-x)\,(D-y)\,F(u_1, u_2)\,(r, n)\,dx\,dy. \tag{9}$$

Vickery further assumed that the lattice plate theory could be applied to solid plates and showed some comparisons of theory with experiment. He measured the function $F(u_1, u_2)\,(r, n)$ behind a grid (similar to the one used in this investigation), and fitted his results with the empirical relation

$$F(u_1, u_2)\,(r, n) = e^{-7\cdot5(\theta/2\pi)} \cos 1\cdot4\pi(\theta/2\pi), \tag{10}$$

where

$$\frac{\theta}{2\pi} = \frac{r}{2\pi Lx}\left[1 + \left(\frac{2\pi nLx}{U}\right)^2\right]^{\frac{1}{2}}.$$

Aerodynamic admittances have been computed, using (9) and (10), and are presented as the full lines in figure 11, for the values of Lx/D investigated in the experiments together with the experimental results for the extreme values of Lx/D. At low values of nD/U there is fairly close agreement with experiment when $Lx/D = 1\cdot5$ but for smaller values of Lx/D the predicted large reduction in $X^2(n)$

is not realized. An alternative form of the co-spectral density function, suggested by Wardlaw & Davenport (1964), is given by the equation

$$F(u_1, u_2)(r, n) = e^{-8nr/U}. \tag{11}$$

Aerodynamic admittances, calculated using (11) are also plotted in figure 11 and show a better agreement with experiment at high values of nD/U. Equation

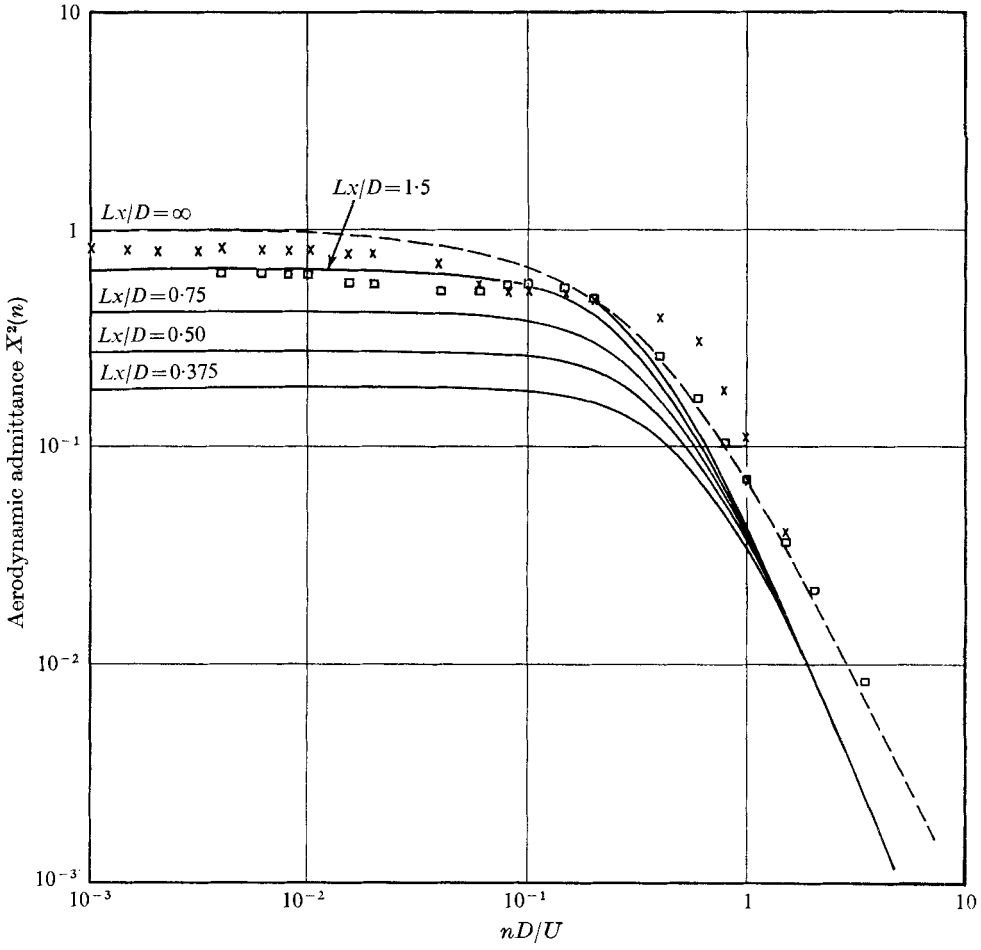

FIGURE 11. Theoretical values of aerodynamic admittance. ×, 2 in. × 2 in., $Lx/D = 1{\cdot}5$; □, 8 in. × 8 in., $Lx/D = 0{\cdot}375$. ——, theory using $F(u_1, u_2)(r, n) = e^{-7{\cdot}5(\theta/2\pi)} \cos 1{\cdot}4\pi(\theta/2\pi)$; – – –, theory using $F(u_1, u_2)(r, n) = e^{-8nr/U}$.

(11), however, gives an incorrect description of isotropic turbulence, particularly at low wave-numbers. The agreement in $X^2(n)$ between theory and experiment at high values of nD/U, may be partly fortuitous because the measurements of power spectral density of drag at these values of nD/U have suggested that the drag fluctuations are not directly related to the upstream velocity fluctuations.

3.7. *Investigation into the structure of the flow around the plates*

The theoretical ideas discussed in the previous section are based on the assumption that there is some correlation between the longitudinal component of the upstream fluctuating velocity and the fluctuating drag. To test this assumption a hot wire was introduced into the flow at various distances, x, ahead of the 4 in.

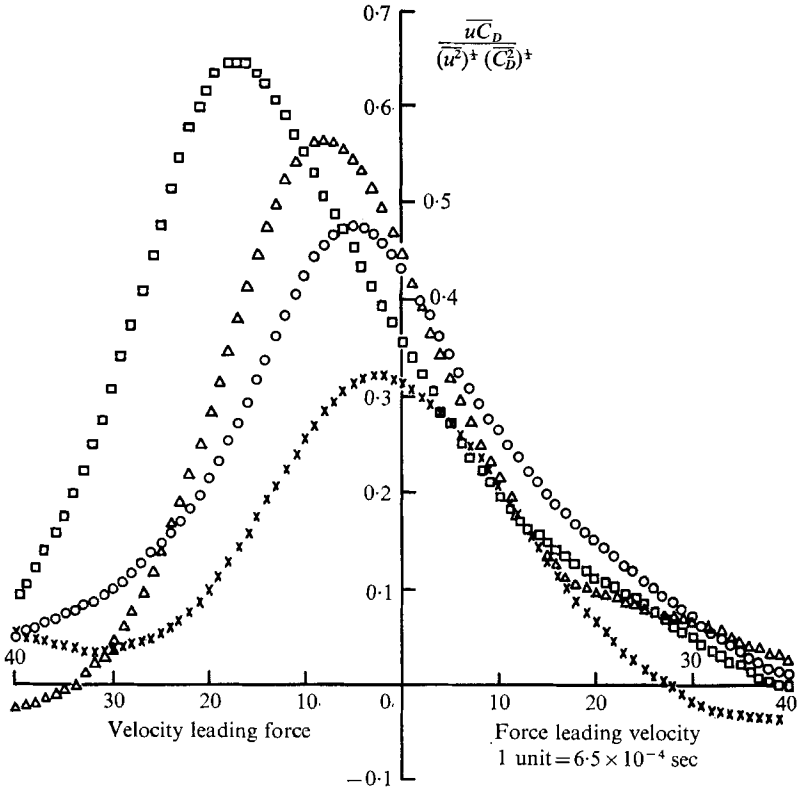

FIGURE 12. Time-delayed cross-correlation between velocity and force. ×, $x/D = 0{\cdot}125$; ○, $x/D = 0{\cdot}25$; △, $x/D = 0{\cdot}5$; □, $x/D = 1{\cdot}0$; $u = 32{\cdot}6$ ft/sec and $Lx/D = 0{\cdot}75$.

square plate, along the stagnation streamline. The fluctuating velocity and fluctuating drag signals were recorded simultaneously and later digitized. The cross-correlation coefficient between velocity and drag force, $\overline{uC_D}/(\overline{u^2})^{\frac{1}{2}}(\overline{C_D^2})^{\frac{1}{2}}$ was computed at various time delays and the results are plotted in figure 12. At each position the maximum correlation occurred when the velocity led the drag force and, as expected, the time delay to maximum correlation increased with distance ahead of the plate. The maximum value of the correlation is shown plotted against position ahead of the plate in figure 13. As x/D tends to zero the correlation will also approach zero because at the plate surface the longitudinal component of the fluctuating velocity must be zero. At $x/D = 1$ the correlation for the whole signal rose to the value 0·65 and, from the slope of the curve, appears to rise even higher further ahead of the plate. The high value of this correlation is surprising when it is remembered that for this plate $Lx/D = 0{\cdot}75$

and the velocity has only been measured at points on the stagnation streamline, whereas fluctuating velocities anywhere over an area of the same order as the size of the plate might affect its drag.

In addition to the unfiltered correlations, figure 13 shows maximum values of time-delayed, filtered cross-correlations for a high and a low value of the frequency parameter nD/U. At the high value there was small correlation and therefore these measurements also help to support the argument that at these values of nD/U most of the drag fluctuations are wake induced. Although at the low value of nD/U the measurements indicate a very strong correlation between drag and upstream velocity the simple linear theory of Vickery underestimates $X^2(n)$, at this value of Lx/D by about 50 %.

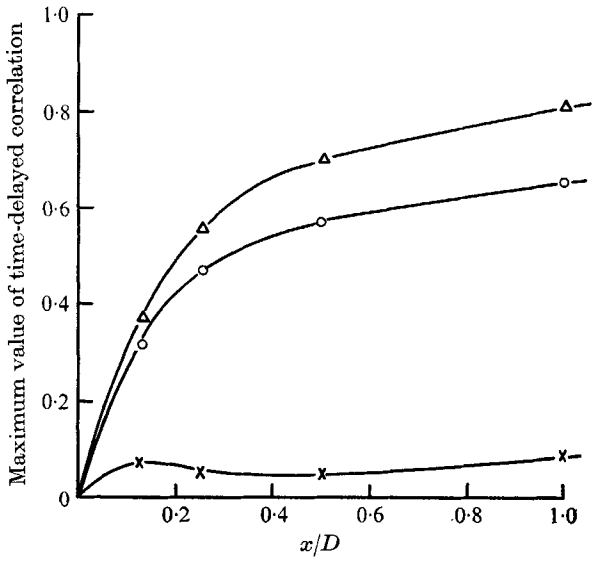

FIGURE 13. Variation of the maximum time-delayed correlation between velocity and drag at various distances ahead of the plate along the mean stagnation line. ○, whole signal; △, $nD/U = 5 \times 10^{-2}$; ×, $nD/U = 1{\cdot}18$.

In order to progress further with the understanding of the effect of turbulence on bodies the effect that the body has on the turbulence must be considered. Hunt (1970) has formulated a theory, based on turbulence rapid distortion theory, to analyze the turbulence in a flow sweeping past a body. Using the ideas of rapid distortion theory it is possible to analyze the effects of a body on the approaching turbulence and thus to obtain a clearer understanding of the mechanism that determines aerodynamic admittance. The principal assumption made in the theory is that, in the time it takes for the turbulence to be swept past the body, the changes in the mean flow around the body and the effects of its boundaries distort the turbulence far more than its own internal viscous and non-linear inertial forces. The turbulence will be distorted by stretching and twisting of the vortex line filaments as they are convected past the body. At this stage no attempt has been made to calculate the distortion of the turbulent flow

ahead of the plates because, when the scale of turbulence is of the same order as the size of the body, the amount of computation required is extremely large. The theoretical ideas will be used, however, to discuss qualitatively the effects of turbulence.

When the eddy sizes of the turbulence are large compared to the size of the body ($Lx/D \to \infty$), the effect of the body on the turbulence will be similar to its effect on the mean flow. Therefore ahead of a plate, along the stagnation streamline, the u' fluctuation will decrease while the turbulence intensity based on local

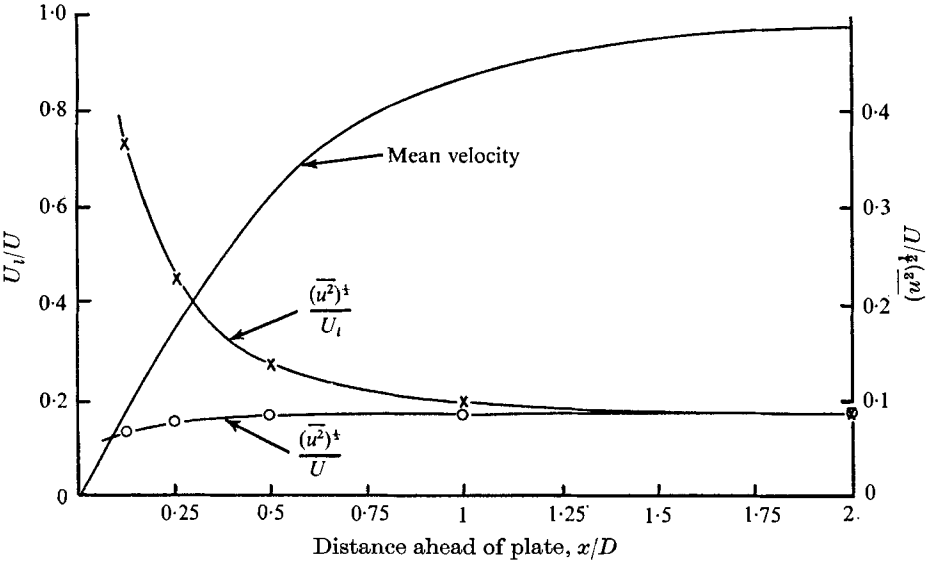

FIGURE 14. Stagnation line flow, $Lx/D = 0{\cdot}75$, $(\overline{u^2})^{\frac{1}{2}}/U = 0{\cdot}083$.

velocity will remain constant. As the plate is approached the u' energy will be transferred into the v' and w' components. On the other hand, as the eddy sizes become very small compared to the size of the body the dominant effect will be the stretching of the vortex lines. This gives the interesting result that, ahead of a plate, u' increases while v' and w' remains almost constant, i.e. the opposite effect to that for the large eddy sizes. When $Lx/D = O(1)$ there will be some combination of these effects.

In order to illustrate some of these features, further measurements along the stagnation line ahead of 4 in. plate are presented. Figure 14 shows measurements of mean velocity, and also the turbulence intensity, based on both local velocity U_l and free stream velocity U, plotted against x/D. The rise in $(\overline{u^2})^{\frac{1}{2}}/U_l$ near the plate suggests that the range of eddy sizes within the turbulence was such as to produce some stretching of the vortex lines. Near the plate, around the stagnation region, very high levels of turbulence intensity were recorded and the accuracy of the hot wire must be considered to be rather low in this area.

The theory of Vickery, when applied to solid plates, assumes that the turbulence approaching each element of plate area behaves as if the body were in a stream where $Lx/D = \infty$. This suggests that along the stagnation streamline

the power spectral density of the approaching flow $F(u)\,(n)_l$ should decrease at all wave-numbers in such a way that

$$F(u)\,(n)_l/U_l^2 = F(u)\,(n)/U^2$$

where $F(u)\,(n)$ is the power spectral density of the fluctuating velocity far upstream. Power spectra of fluctuating velocity along the stagnation streamline

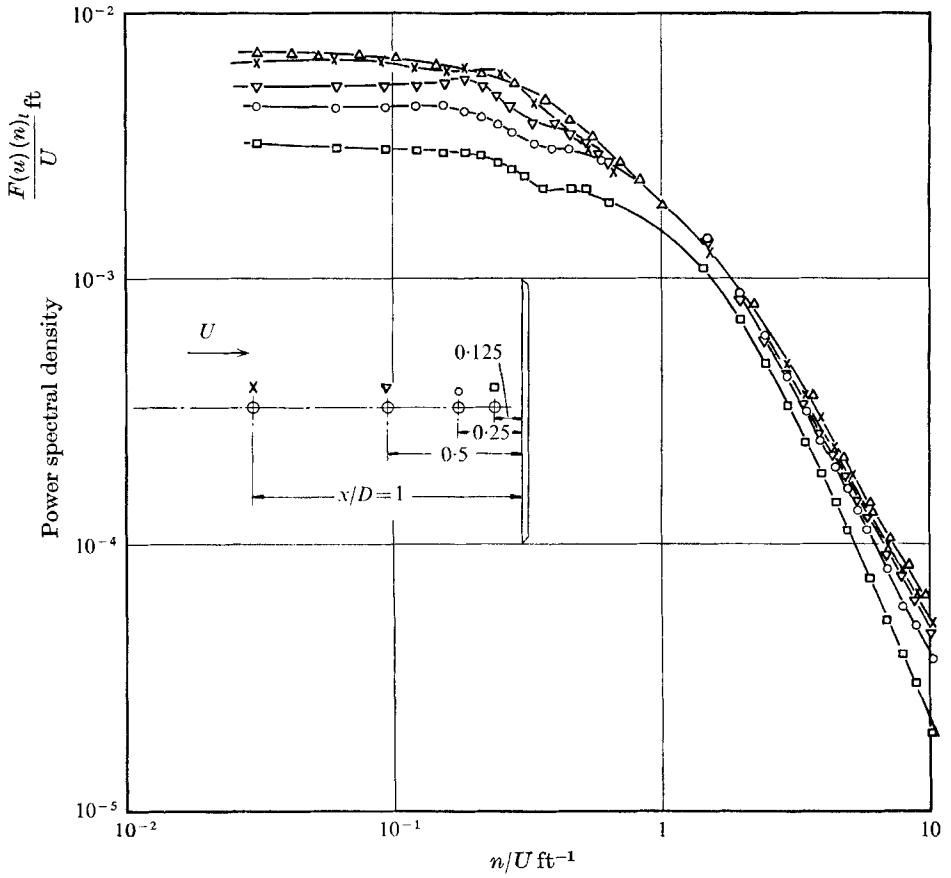

FIGURE 15. Spectra of velocity fluctuations along the stagnation line.
△, free stream in absence of plate.

at four stations ahead of the plate are shown in figure 15. $F(u)\,(n)_l/U$ is shown plotted against n/U and the area under each spectrum is equal to the square of the turbulence intensity based on free stream velocity. Compared with the spectrum in the absence of the plate, the power $F(u)\,(n)_l/U$ at low wave-numbers shows a decrease, whereas at higher wave-numbers there is little change. If $Lx/D = \infty$ and there was no stretching of vortex lines by the mean flow the level of the spectrum at all wave-numbers would be given by equation (12).

$$\frac{F(u)\,(n)_l}{U} = \frac{F(u)\,(n)}{U}\frac{\overline{U}_l^2}{\overline{U}^2}. \tag{12}$$

Taking as an example a value of $n/U = 3 \times 10^{-2}$ at $x/D = 0{\cdot}25$, where (from figure 14) $U_l/U = 0{\cdot}35$, (12) gives $F(u)\,(n)_l/F(u)\,(n) = 0{\cdot}12$. The measurements in figure 15, however, show $F(u)\,(n)_l/F(u)\,(n) = 0{\cdot}62$. At high wave-numbers the effect of distortion by the mean flow is even more marked.

Returning to the theoretical values of aerodynamic admittance plotted in figure 11 it can be seen that as Lx/D decreases $X^2(n)$ becomes increasingly larger than Vickery predicts. This is perhaps in agreement with the finding that as Lx/D becomes smaller the distortion of the turbulence intensifies the longitudinal component of turbulence ahead of the body. More work is required to determine the importance of turbulence distortion and to determine whether, if Lx/D is large enough, the much simpler ideas of Vickery are sufficient to predict $X^2(n)$ accurately at low values of nD/U. It is interesting to note that when $Lx/D = 1{\cdot}5$ the aerodynamic admittance values predicted by Vickery are only 20 % too low. Another area requiring more attention is the understanding of the complex interaction between the turbulence and the wake.

4. Conclusions

The time mean base pressure measured on square and circular plates in turbulent flow was found to be considerably lower than that measured in smooth flow. It is suggested that the principal reason for this is that, compared to smooth flow, there is extra entrainment of fluid out of the wake resulting from the mixing of the near wake with the free stream turbulence. In support of this argument, the measurements of base pressure coefficient are shown to correlate well with the turbulence parameter $[(\overline{u^2})^{\frac{1}{2}}/U]\,Lx^2/A$.

Power spectral density measurements of the fluctuating drag on square plates in turbulent flow show the importance of the scale parameter Lx/D. As Lx/D increases, the correlation areas of the energy containing eddies of the turbulence are comparatively larger and the root-mean-square value of the drag coefficient fluctuations increases. Correlations of the velocity signal from a hot wire, placed at various distances upstream of a plate ($Lx/D = 0{\cdot}75$), with the fluctuating drag signal confirmed that the majority of the drag fluctuations was linearly related to the velocity fluctuations in the approaching flow. This relationship between velocity and drag helps to justify, particularly at values of nD/U less than 0·1, the concept of aerodynamic admittance. In the range of values of Lx/D from 1·5 to 0·375, however, the theory of Vickery, at small nD/U, was found to underestimate seriously the value of aerodynamic admittance. Measurements of the structure of the turbulence ahead of a plate suggest that this was primarily due to the significant distortion of the turbulence by the body.

The measurements suggest a further contribution to drag fluctuations, uncorrelated with upstream velocity, perhaps resulting from wake-induced pressure fluctuations on the rear face. Comparisons of drag spectra show that, at high values of nD/U power spectral density decreases with increasing nD/U at the same rate in turbulent flow as in smooth flow. The level of the spectra in turbulent flow at the same value of nD/U, however, are nearly three orders greater.

Thanks are due to Mr G. S. Smith for the design of the drag balance. The work described in this paper, which was carried out as part of the general research programme of the National Physical Laboratory, was supported in part by the Construction Industry Research and Information Association.

REFERENCES

BEARMAN, P. W. 1969 *Nat. Phys. Lab. Aero. Rep.* no. 1296.
DAVENPORT, A. G. 1961 *Proc. Inst. Civ. Engrs* **19**, 449–472.
FAIL, R., LAWFORD, A. & EYRE, R. C. W. 1955 *Aero. Res. Coun. R. & M.* no. 3078.
HUNT, J. C. R. 1970 A theory of turbulent flow over bodies. To be published.
MASKELL, E. C. 1965 *Aero. Res. Coun. R. & M.* no. 3400.
SCHUBAUER, G. B. & DRYDEN, H. L. 1935 *NACA Rep.* no. 546.
VICKERY, B. J. 1965 *Nat. Phys. Lab. Aero. Rep.* no. 1143.
WARDLAW, R. L. & DAVENPORT, A. G. 1964 *Nat. Res. Coun. of Canada. Aero. Rep.* LR–416.